

INFLUENCE OF ANNEALING TEMPERATURE ON STRUCTURAL AND MORPHOLOGICAL PROPERTIES OF MANGANESE OXIDE (Mn_2O_3)

N. R. CHANDAR^{a,*}, S. AGILAN^b, N. MUTHUKUMARASAMY^b, R. GANESH^c

^aDepartment of Physics, Hindusthan Institute of Technology, Coimbatore, India

^bDepartment of Physics, Coimbatore Institute of Technology, Coimbatore, India

^cDepartment of Physics, RVS College of Engineering and Technology, Coimbatore, India

Manganese oxide (Mn_2O_3) nanoparticles have been synthesized in co-precipitation method and followed by annealing of the samples at 200°C, 400°C and 600°C at 10 hours. The prepared samples are characterized with X-ray diffraction (XRD), scanning electron microscopy (SEM), energy dispersive analysis of X-ray spectroscopy (EDAX), UV-visible spectroscopy and vibrating-sample magnetometer (VSM). The XRD spectra reveals that the body centred cubic structure of Mn_2O_3 powder was obtained. Annealing temperature proliferates the crystallite sizes from 31 to 81nm are calculated by Scherer's formula. The SEM image unveils that the materials have an irregular nano-stick like morphology. Optical properties are appraised by UV-visible spectroscopy; band gap values deceased with increasing annealing treatment. Low annealing temperature treatment sample shows high transmittance in visible region. FT-IR studies shows that the number of surface hydroxyl group dwindle with the enhance of annealing temperature. The magnetization (VSM) is conducted to the sample and the saturation magnetization (M_s) is 38.73emu/g.

(Received June 27, 2018; Accepted November 23, 2018)

Keywords: Nanostructures, Oxides, Chemical synthesis and structural characterization

1. Introduction

A great concentration has been paid in developing nanomaterials based on the transition metal oxides due to their structural flexibility combined with novel chemical and physical properties (1, 2). These properties coming out from the electronic structure and surface to volume ratio in the nano metre regime are strongly related to their size (3, 4). Among the transition metals, manganese has many oxidation states (+2, +3, +4) and forms variety of oxides like MnO , MnO_2 , Mn_2O_3 , Mn_3O_4 and Mn_5O_8 . For that reason, it has attracted significant research efforts (5). It has wide range of applications in catalytic, electrochemical, magnetic, optical and electro catalytic bio sensors (6). Especially, Mn_2O_3 has attracted much interest as an anode material in the lithium ion battery and can also be used for preparing soft magnetic materials such as manganese zinc ferrite (7).

The present research work represents the impact of annealing temperature on the morphology and size of Mn_2O_3 particles synthesised in co-precipitation method. As synthesized Mn_2O_3 particles were annealed at 200°C, 400°C and 600°C at 10 hours. The structural, surface morphology and elemental composition of the samples were characterized by XRD, SEM and EDAX techniques. And magnetic properties of the samples were studied using VSM method.

2. Synthesis of manganese oxide nano particles

Nano sized Mn_2O_3 particles were synthesized in co-precipitation method. In the synthesis 0.1M of sodium hydroxide was added drop wise into the 0.1 M Manganese chloride solution with constant stirred. The mixture was then heated at 60°C for 2 hrs for the completion of the reaction.

* Corresponding author: saranspectra@gmail.com

The products obtained were separated by filtration and washed several times in distilled water to free it from ions and other impurities. It was dried at 60°C for 5 hours and the powder obtained was annealed at 200°C, 400°C and 600°C at 10 hrs in a muffle furnace to obtain nano powder of manganese oxide.

The powder samples were characterized by X-ray diffractometer using Cu-K-alpha radiation ($\lambda = 1.5406 \text{ \AA}$) in range $10^\circ \leq 2\theta \leq 80^\circ$. The X-ray tube used was a copper tube operating at 30KV and 30mA. The surface morphology of the powdered samples was obtained by FE-SEM. FT-IR spectra of the samples were recorded in the range 4000 cm^{-1} to 400 cm^{-1} in order to confirm the formation of expected oxide and to check the purity. The magnetic study was conducted with vibrating sample Magnetometer with a moment measurement range of 3.1×10^{-6} emu to 1000emu.

3. Results and discussions

3.1 Structural analysis

The XRD patterns of various annealing temperature samples are illustrated in Fig. 1. The results show that the sample annealed at 200°C has diffraction peaks at 2θ values 32.9° , 38.6° , 45.0° , 59.0° , 60.4° and 65.2° which corresponds (222), (400), (332), (600), (611) and (622) planes respectively. This illustrates that the powder grew in the cubic structure which is in a good agreement with early reported (10). Similarly in the XRD of the sample annealed at 400°C the diffraction peaks at 2θ values 38.6° , 46.4° , 49.7° , 55.2° , 60.4° and 66.2° has been observed which corresponds (400), (431), (431), (440), (611) and (622) planes respectively and the cubic structure. Additional peaks were observed at $2\theta = 23.59^\circ$ (211) and $2\theta = 33.36^\circ$ (222) matched with JCPDS card no: 01-1061. In the diffraction pattern of sample annealed at 600°C peaks were observed at 35.7° , 38.3° , 45.2° , 49.4° , 60.4° and 65.2° which corresponds to the planes (321), (400), (332), (431), (611) and (440) of Mn_2O_3 particles compared to the standard peaks of pure Mn_2O_3 (JCPDS 041-1442) and also the additional peaks are observed as similar as in 400°C. From the analysis, the annealing temperature can be enhanced the additional peaks intensity and become more sharper due to its powders are in good crystallinity (8, 12)

The hkl planes are well indexed to the cubic phase with lattice parameter $a = 9.4091 \text{ \AA}$ which was calculated using the combined formula of Bragg and interplaner distance of the cubic structure as in equation (9). This value is more or less equal to all the annealing temperature.

$$a = \lambda \sqrt{\frac{h^2 + k^2 + l^2}{2 \sin \theta}} \quad (1)$$

This result is in good accordance with JCPDS (89-4836) and early reported by thota et.al (10). The average crystalline size estimated using Debye- Scherer's formula (11).

$$\cos \theta = \frac{k\lambda}{D} \times \frac{1}{\beta_{hkl}} \quad (2)$$

where $k = 0.9$ is the shape factor λ is the x-ray wavelength β is the full width at half maximum in radians and θ is the angle position of the maximum of diffraction peak. By using the above equation, the average crystalline size was estimated for 200°C, 400°C and 600°C to be estimated about 31.3nm, 39.5nm and 81.3nm respectively, which indicates the crystalline size is improved with increasing annealing temperature (12)

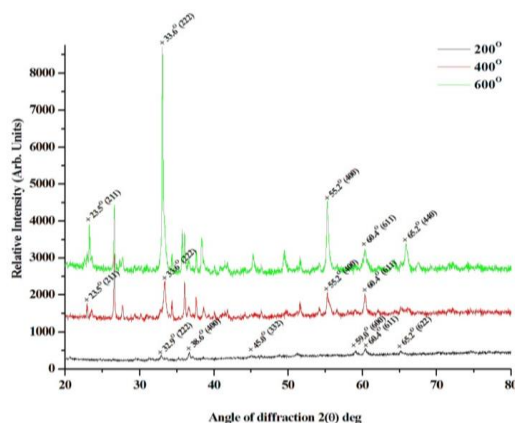


Fig. 1. Powder X-ray diffraction patterns of the Mn_2O_3 samples annealed at different temperatures.

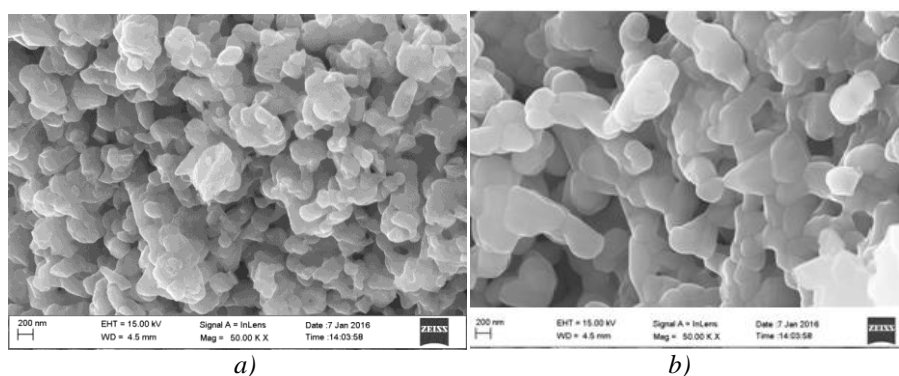


Fig. 2. FE-SEM images of the Mn_2O_3 annealed at (a) 200°C and (b) 600°C.

The surface morphology of the annealing Mn_2O_3 powder is examined by FE-SEM and the results obtained are shown in the Fig. 2. The images show that the materials annealed at 200 °C have an irregular stick like morphology. The particles size of the samples are 184 nm and 193 nm at 200°C and 600°C respectively, this shows that the higher annealing temperature is enhanced the particle size (13) owing to surface area of the material is decreased. Comparing the images there is no change in structure/surface smoothness of the sample.

The elemental spectra of manganese oxide powder are presented in Fig. 3. It confirms the presence of Mn and O elements in the powder. The atomic percentage of Mn and O elements in the Mn_2O_3 samples was nearly 36 % and 59 % respectively. The higher percentage of ‘O’ in the EDAX analysis results might be due to the presence of adsorbed water molecules in the surface of the Mn_2O_3 samples.

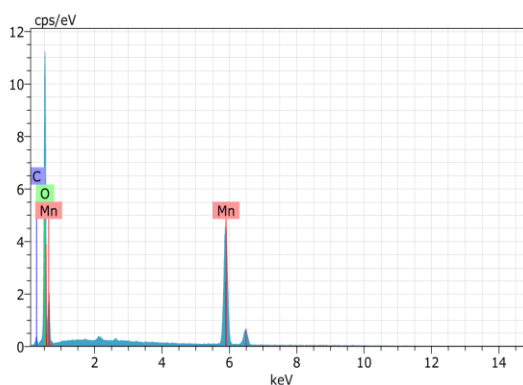


Fig. 3. EDAX spectra of the Mn_2O_3 sample.

3.2 UV- visible analysis

Fig. 4 shows the transmittance of manganese oxide powder sample annealed at various temperatures. From figure 4 the prepared powders are having mounting transparency in the visible region (200-800nm) and manganese oxide powder annealed at low temperature exhibit highest transmittance of 70-85% compared with other samples which means the annealing temperature has on impact on it due to increasing grain size of manganese oxide powder (14). Transmittance intensity is reduced with increasing annealing temperature owing to the improvement of grain size (15)

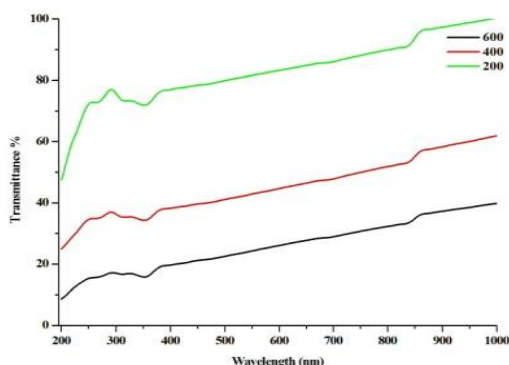


Fig. 4. UV-Vis Transmittance spectra of manganese oxide nano particles annealed at different temperatures.

The band gaps (E_g) of the materials have been calculated from the plot of $(\alpha h\nu)^2$ Vs $h\nu$ as proposed by the Wood and Tauc(16) and the results are presented in the Fig. 5. The relationship between $\alpha h\nu$ and band gap (E_g) given in following equation,

$$(\alpha h\nu) \propto (h\nu - E_g)^n \quad (3)$$

where ' α ' is the absorbance, ' h ' is the Planck constant, ' ν ' is the frequency, ' E_g ' is the optical energy band gap and ' n ' is a constant associated to the different types of electronic transitions ($n=1/2, 2, 3/2$ or 3 for direct allowed, indirect allowed, direct forbidden and indirect forbidden transitions, respectively).

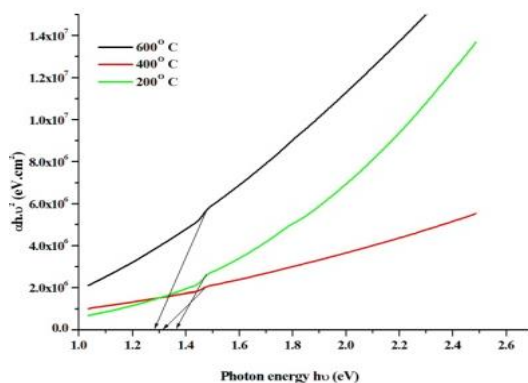


Fig. 5 $(\alpha h\nu)^2$ versus $h\nu$ in eV of prepared samples at different annealing temperatures.

The calculated bandgap of the samples are 1.36, 1.32 and 1.29 eV 200°C, 400°C and 600°C respectively. This shows that the increase of annealing temperature reduces the band gap energy. The decrease in band gap energy of the materials might be due to its increased particle

size at higher annealing temperature (17). The influence of annealing temperature on particle size is already presented in XRD studies.

3.3 FTIR Spectral studies

The spectra of three samples of Mn_2O_3 nanoparticles synthesized by co-precipitation method and annealed at 200 °C, 400 °C and 600 °C are given in Fig.6. In the spectrum of the sample annealed at 200°C, the peaks appearing at 617 and 493 cm^{-1} correspond to the stretching vibration of Mn–O and Mn–O–Mn bonds indicating the formation of Mn_2O_3 .

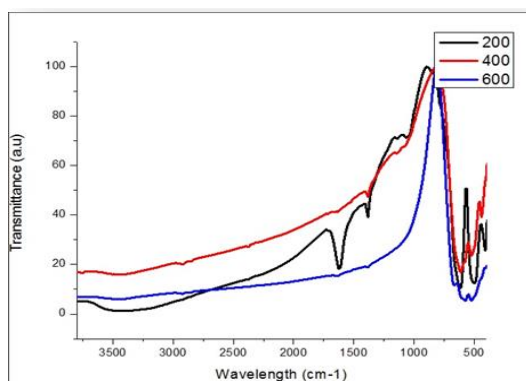


Fig. 6. FTIR spectra of manganese oxide nanoparticles annealed at different temperatures.

These two characteristic peaks appeared at 609 cm^{-1} and 524 cm^{-1} in the sample annealed at 400 °C and whereas in the sample annealed at 600 °C they were found at 663 and 578 cm^{-1} (18) showing isomorphism among the three samples. In all the samples a peak with weak intensity and is observed around 3400 cm^{-1} resulting from O-H stretching vibration of uncondensed surface hydroxyl groups and water molecule (19). The origin of this peak may be due to absorption of moisture from the atmosphere. An important observation from close analysis of the spectra is that the O-H peak becomes weak when the annealing temperature is raised. Thus it can be inferred that the hygroscopicity of the metal oxide nanoparticles decreases with increasing annealing temperature. Since the method of preparation of the nanoparticles did not involve any organic moieties, the spectra did not show any specific organic functional groups except in the sample annealed at 200 °C. This sample displays two peaks at 1620 and 1380 cm^{-1} , which may be due to absorption of impurities during recording the spectrum.

3.4 Magnetic studies

The magnetic properties of the Mn_2O_3 can be explained in terms of the cations distribution. Magnetization originates from divalent metal (M^{2+}) ions in tetrahedral sites and M^{3+} ions in octahedral sites (20). The magnetic studies of Mn_2O_3 nanoparticles were performed using the vibrating sample magnetometer (VSM) and the result of hysteresis curves of the Manganite nanoparticles are shown in Fig.7 at 300 K temperature. The magnetic hysteresis loops were measured under a maximum applied field of 1.5 T at room temperature to determine magnetic parameters such as saturation magnetization (M_s), coercivity (H_c), magnetic retentivity (M_r).

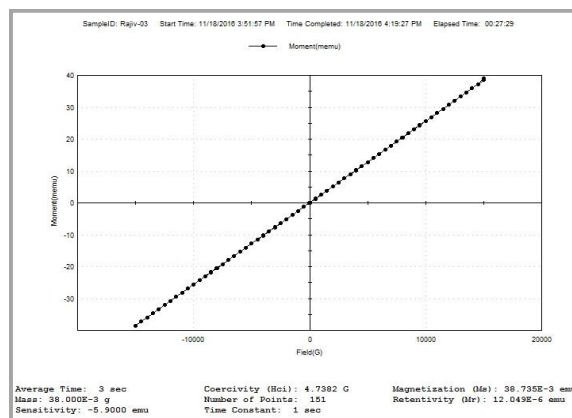


Fig.7. VSM study of manganese oxide nanoparticles annealed at 600 °C.

In the present study, the magnetite nanoparticles calcinated at 600 °C were taken for magnetic hysteresis curves measurement. The hysteresis loop measurement at room temperature (300 K), the coercivity (H_c) of Mn_2O_3 is 4.7382 Gauss and saturation magnetization (M_s) is 38.735 emu/g. The values of the remanent ratio ($M_r/M_s = 0.311$) of the prepared samples are high and indicative of the anisotropic nature of the materials. The surface effect may be developed due to the existence of an inactive magnetic layer or a disordered layer on the surface of nanoparticles and the heating rate of calcinations. It appears that as the annealing temperature increases, occupation ratio of manganese ions at octahedral sites decreases and hence, magnetic moment of Mn_2O_3 nanoparticle is enhanced as compared to literature value (21).

Fig. 7 shows the magnetic behaviour of Mn_2O_3 nanoparticles annealed at 600°C. The magnetic study has been carried out in ambient temperature with maximum magnetic field at koe. The annealed Mn_2O_3 particles exhibited paramagnetic behaviour (14) and the—maximum magnetization was observed at 38.73-emu/g.

4. Conclusions

Mn_2O_3 nanoparticles were synthesized in co-precipitation method, through which Annealing of the synthesised material was found to enhance its crystallinity and particle size. The formation of body centred cubic phase crystalline structure of Mn_2O_3 was confirmed by the powder XRD analysis. XRD revealed the new peaks for annealed samples with the same structure and also indicated the increase in crystallinity.

FE-SEM exposed the size of the particle were 184 nm and 193nm at 200°C and 600°C respectively. The chemical composition and purity of the samples were examined by EDAX and the contradictory results were found. Magnetic studies confirmed that the paramagnetic behaviour of Mn_2O_3 nanoparticles and improved for annealed samples due to increase in crystallinity.

References

- [1] G. J. Moore, R. Portal, A. Le Gal La Salle, D. Guyomard, J. Power sources **97**, 393 (2001).
- [2] M. M.Thackeray, S. H. Kang, C. S. Johnson, J. T. Vaughley, R. Bendek, S. A. Hackney, J. Mater. Chem. **17**, 3112 (2007).
- [3] M. L. Steigerwald, L. E. Brus, Acc. Chem. Res. **23**, 183 (1990).
- [4] A. P. Alivisatos, J. Phys. chem., 100 (1996).
- [5] J. Euna, K. Changsoo, L. Soonchil, New j. Ohys. **13**, 013018 (2011) .
- [6] R. Jothiramalingam, M. K. Wang, J. Porous. Mater. **17**, 677 (2001).
- [7] Chugai Electric Industrial Co.Ltd, Jpn. KoKai Tokyo Koho. JP 02.35915[90,35,915],

- February 6 (1990).
- [8] B. Gillot, M. El Guendouzi, M. Laarj, *Materials chemistry and physics* **70**, 54 (2001).
- [9] Irene Rusakova, Teyeb Ould-Ely, Cristina Hofmann, Dario Prieto-Centurion, Carly S. Levin, Naomi J. Halas, Andreas Luttge, Kenton, H. Whitmire, *Chemistry of materials* **19**, 1369 (2007).
- [10] Z. Yang, Y. Zhang, X. Wang, Y. Qian, X. Wen, S. Yang, *Journal of solid state chemistry* **17**, 679006).
- [11] Alejandra Ramirez, Philipp Hillebrand, Diana Stellmach, M. Mathius, Peter May, Sebastian Fiechter, *J. Phys. Chem. C* **118**, 14073 (2014).
- [12] Qurat-ul-ain Javed, Wang Feng-Ping, M. Yasir Rafique, Arbab Mohammad Touiq, Zubir Iqbal, *Chin. Phys. B Vol.* **21**(11), 117311 (2012).
- [13] T. Shrividhya, G. Ravi, T. Mahalingam, Hayakawa Synthesis and Study on Structural, Morphological and Magnetic properties of nanocrystalline Manganese Oxide, *International Journal of Science and Engineering Applications, Special Issue NCRTAM ISSN-2319-7560*.
- [14] N. Ponpandian, Narayanasamy, C. N. Chinnasamy, N. Sivakumar, *Appl. phys. lett.* **86**, 192510 (2005).
- [15] B. M. Pradeep Kumar, K. H. Shivaprasad, R. S. Raveendra, R. Hari Krishna, Sriram Karikkat, B. M. Nagabhushana, *International Journal of Application or Innovation in Engineering & Management (IJAIEM)* **3**(12), 102 (2014).
- [16] V. Mohanraj, R. Jayaprakash, J. Chandrasekaran, R. Robert, P. Sangaiya, *Materials Science in Semiconductor Processing* **66**, 131 (2017).
- [17] C. Hongmin, H. abd Junhui, *The Journal of Physical Chemistry C* **112**, 17540 (2008).
- [18] Majed Sharrouf, Ramadan Awad, Mohamad Roumie, Salem Marahaba, *Materials Science and Applications* **16**, 850 (2015).
- [19] Z. W. Chen, S. Y. Zhang, S. Tan, F. Q. S. Li, J. Wang, S. Z. Jin, Y. H. Zhang, *Journal of Crystal Growth* **80**, 280 (1997).
- [20] Jr-Ivan Lai, Kurikka V. P. M Shufi, Abraham Ulman, Nan-Loh Yang, Min-Hui- Lui, Thomas Vogt, Claude Estournes, *Chem. Soc. Div. Fuelchem* **48**(2), 729 (2003).
- [21] Stephen Blundell, *Magnetism in Condensed Matter, Firsted., Oxford University Press Inc., New York*, 2001.
- [22] D. Yan, S. Cheng, R. F. Zhuo, J. T. Chen, J. J. Feng, H. T. Feng, H. J. Li, Z. G. Win, J. Wang, X. P. Yan, *Nanotechnol.* **20**, 105706 (2009).
- [23] W. L. He, Y. Zhang, X. Zhang, H. Wang, H. Yan, *J. Cryst. Growth* **252**, 285 (2003).
- [24] M. Nieberberger, *Acc. chem. Res.* **40** (2007).
- [25] M. M. Titirici, M. Antonietti, A. Thomas, *Chem.* **109**, 1125 (2005).
- [26] S. Gnanam, V. Rajendran, *J. Sol- Gel Sci. Technol.* **58**, 62 (2011).
- [27] R. Ramachandran, *Journal of Materials Science –Materials in Electronics* **13**, 257 (2002).
- [28] M. Roumie, B. Nsouli, K. Zahraman, A. J. Reslan, *Nucl. Instr. Meth B* **389**, 219 (2004).
- [29] S. Thota, B. Prasad, J. Kumar, *Materials Science and Engineering B* **167**, 153 (2010).
- [30] A. A. Audi, P. M. A. Sherwood, *Surf. Interface Anal.* **33**, 274 (2002).
- [31] R. K. Sharma, A. C. Rastogi, S. B. Desu, *Electrochim. Acta* **53**, 7690 (2007).